First-principles and semi-empirical van der Waals study of thymine on Cu(110) surface

V. Caciuc,[1,2,*] N. Atodiresei,[2,3,†] P. Lazić[‡],[2] Y. Morikawa,[3] and S. Blügel[2]

[1] *Physikalisches Institut, Westfälische Wilhelms Universität Münster, Wilhelm-Klemm-Str. 10, 48149 Münster, Germany*

[2] *Institut für Festkörperforschung (IFF), Forschungszentrum Jülich, 52425 Jülich, Germany*

[3] *The Institute of Scientific and Industrial Research, Osaka University, 8-1 Mihogaoka, Ibaraki Osaka, 567-0047 Japan*

(Dated: August 12, 2013)

In this study we investigated by means of density functional theory calculations the adsorption geometry and bonding mechanism of a single thymine ($C_5H_6N_2O_2$) molecule on Cu(110) surface. In the most stable energetic configuration, the molecular plane is oriented perpendicular to substrate along the $[1\bar{1}0]$ direction. For this adsorption geometry, the thymine molecule interacts with the surface via a deprotonated nitrogen atom and two oxygen ones such that the bonding mechanism involves a strong hybridization between the highest occupied molecular orbitals (HOMOs) and the *d*-states of the substrate. In the case of a parallel adsorption geometry, the long-range van der Waals interactions play an important role on both the molecule-surface geometry and adsorption energy. Their specific role was analyzed by means of a semi-empirical and the seamless methods. In particular, for a planar configuration, the inclusion of the dispersion effects dramatically changes the character of the adsorption process from physisorption to chemisorption. Finally, we predict the real-space topography of the molecule-surface interface by simulating scanning tunneling microscopy (STM) images. From these simulations we anticipate that only certain adsorption geometries can be imaged in STM experiments.

PACS numbers: 71.15.Dx 68.43.-h 68.43.Bc 68.43.Fg

I. INTRODUCTION

The development of electronic devices like organic light-emitting diodes (OLEDs)[1,2] has opened the road to an alternative technology to the silicon-based one to manufacture integrated electronic devices built on single molecules. Nowadays, the emerging field of molecular electronics[3,4] focuses on the possibility of using organic molecules adsorbed on surfaces as basic functional units to construct technological relevant electronic devices such as single molecule diodes,[5,6,7] organic field-effect transistors[8,9,10] or ultra-high-density memory circuits.[11]

A very appealing feature of molecular devices is the prospect of tuning their physical properties at atomic scale by chemical functionalization of the molecule-surface interface under consideration. A key aspect of this approach is to employ molecules with several functional groups that adsorb on surface through one such group while the others can be used to react with other molecules to selectively modify the geometry and electronic properties of adsorbate-substrates systems. For instance, experimental studies aimed to investigate the functionalization of the Cu(110) surface by adsorption of organic molecules have been performed for terephthalic[12] and oxalic[13] acids.

In this context, the chemical functionalization of surfaces via biologically relevant molecules is of particular interest due to the potentially important applications such as molecular biosensors.[14,15,16] In particular, one of the most important molecules in biology is thymine ($C_5H_6N_2O_2$). Its importance stems from the fact that it is a fundamental nucleobase of the deoxyribonucleic acid (DNA) and encodes genetic information by pairing with the adenine base. The adsorption of thymine on surfaces is then of particular interest since it represents a possible channel for anchoring of DNA on substrates. The relevance of this process is also highlighted by the observation that the thymine base is absent in the case of the ribonucleic acid (RNA).

From experimental point of view, the adsorption process of thymine on Cu(110) surface was intensively investigated by means of reflection-adsorption infrared spectroscopy (RAIRS),[17,18] (soft-)X-ray photoelectron spectroscopy (XPS),[19,20] near-edge X-Ray adsorption fine structure (NEXAFS)[19,20] and photoelectron diffraction[20] at room or higher temperatures. These studies suggest that, in the limit of low coverage, the geometry of the thymine-Cu(110) system corresponds to an upright orientation of the molecular plane aligned along $[1\bar{1}0]$ surface direction. However, the chemical identity of the functional groups involved in the bonding with the metal substrate is less clear. One possibility is to consider that the thymine molecule binds to Cu(110) surface via a (dehydrogenated) N atom adjacent to two carbonyl groups (CO) while another possible adsorption geometry implies a adsorbate-substrate interaction through the imino (CNH) and carbonyl (CO) groups.

In consequence, in the present study we focus on an *ab initio* investigation of the adsorption geometry and bonding mechanism of a single thymine molecule on Cu(110)

[‡] On leave of absence from the Rudjer Bošković Institute, Zagreb, Croatia.

surface. The bonding geometry of the adsorbed molecule was analyzed as a function of the orientation of the molecular plane with respect to substrate. More specifically, we considered the case when the heterocyclic ring is perpendicular to surface and aligned along its [001] and [1$\bar{1}$0] directions. We also examined a parallel adsorption geometry such that the molecular plane lies flat on surface. In particular, for this bonding geometry the long-range van der Waals interactions are important from geometrical and energetic point of view. The effect of the dispersion corrections on the adsorption geometry was taken into account by means of a semi-empirical approach while their impact on the adsorption energy was also evaluated within the seamless (vdW-DF) method. Besides this, the bonding mechanism of the thymine-Cu(110) system in the perpendicular adsorption geometry was investigated considering a single and double deprotonated $C_5H_6N_2O_2$ at N sites. In each case, we considered two scenarios for the bonding functional groups as already discussed above. The experimental fingerprints of all adsorption geometries analyzed in our study as revealed by scanning tunneling microscope (STM) was also simulated.

II. THEORETICAL METHOD

Our *ab initio* study was performed within the framework of density functional theory (DFT)[21] by using the generalized gradient approximation (GGA) for the exchange-correlation energy functional in the form proposed by Perdew-Burke-Ernzerhof (PBE).[22] The Kohn-Sham equations[23] have been solved self-consistently using the pseudopotential method[24] as implemented in the VASP program.[25,26] The electron-ion interactions are replaced by pseudopotentials described by the projector augmented-wave method (PAW).[27]

The thymine–Cu(110) system was modeled by a periodic slab geometry using the theoretical lattice parameter of the bulk Cu (3.64 Å). In each supercell, the slab consists of five atomic layers separated by a vacuum region of $\approx$ 21 Å. The size of the in-plane surface unit cell was set to 5×4. For this geometrical setup, the Kohn-Sham orbitals were expanded over a plane-wave basis set which includes all plane waves up to a cutoff energy E_{cut} of 450 eV. The geometry of the thymine–Cu(110) system was optimized by relaxing the atomic positions of all molecule atoms and those in two surface layers. The equilibrium geometry of the molecule-Cu(110) surface was obtained when the calculated Hellmann-Feynman forces were smaller than $\approx$ 0.001 eV/Å. Finally, the Brillouin zone integrations were carried out using only the Γ-point.

To investigate the structural stability of different conformational geometries of a single or double deprotonated adsorbate-surface systems, we calculated the adsorption energy E_{ads} and adsorption enthalpy $\Delta H^{ads}_{T=0}$ at a temperature T of 0 K for each geometry under consideration.

The adsorption energy E_{ads} is given by

$$E_{ads} = E_{sys} - E_{Cu(110)} - E_{molecule}. \quad (1)$$

where E_{sys} represents the total energy of the adsorbed thymine-Cu(110) surface system, $E_{Cu(110)}$ is energy of the isolated Cu(110) surface and $E_{molecule}$ denotes the energies of the isolated thymine molecular species as follows: (i) $E_{Thymine}$ −thymine and (ii) $E^{H,H_2}_{Thymine}$ −single (superscript H) or −double (superscript H_2) deprotonated thymine molecule, respectively.

The adsorption enthalpy $\Delta H^{ads}_{T=0}$ is defined as the difference between the sum of the product energies (E_{sys} and E_{H_2} −the total energy of the isolated hydrogen molecule H_2) and the sum of reactant energies ($E_{Cu(110)}$ and $E_{Thymine}$). Therefore, the adsorption enthalpy $\Delta H^{ads}_{T=0}$ is defined by

$$\begin{aligned}\Delta H^{ads}_{T=0} =&(E_{sys} + factor * E_{H_2})- \\ &(E_{Thymine} + E_{Cu(110)}).\end{aligned} \quad (2)$$

where $factor$ is equal 0.0 (for thymine molecule), 0.5 (for a single deprotonated case) or to 1.0 (for a double deprotonated thymine molecule). A negative adsorption enthalpy indicates an exothermic reaction between the thymine molecule and the Cu(110) surface while a positive value of $\Delta H^{ads}_{T=0}$ implies that such reaction is endothermic and requires external energy to make it possible.

However, the double deprotonation process of the $C_5H_6N_2O_2$ molecule can take place through an intermediate step involving a single deprotonated thymine molecule. Two different scenarios are conceivable: (i) the single deprotonated molecule adsorbed on the Cu(110) surface loses one of its proton such that the adsorption enthalpy is given by

$$\Delta H^{ads}_{T=0} = (E^{H_2}_{sys} + 0.5 * E_{H_2}) - E^{H}_{sys}. \quad (3)$$

and (ii) a single deprotonated thymine species in gas phase adsorbs on the metal substrate where undergoes a second deprotonation such that

$$\begin{aligned}\Delta H^{ads}_{T=0} =&(E^{H_2}_{sys} + 0.5 * E_{H_2})- \\ &(E^{H}_{Thymine} + E_{Cu(110)}).\end{aligned} \quad (4)$$

Thus, the adsorption enthalpy $\Delta H^{ads}_{T=0}$ calculated for a double deprotonated $C_5H_6N_2O_2$ molecule by Eqs. 2, 3 and 4 will allow us to get a hint on the details of the deprotonation process of this molecule on Cu(110) surface.

An important question arising when studying the adsorption process of molecules on metal surfaces concerns the role of long-range van der Waals interactions on the geometry and the adsorption energy of the adsorbate-substrate system in question. We addressed this problem in our study by investigating the thymine molecule on Cu(110) surface also in the framework of the semi-empirical approach (DFT-D) as proposed by Grimme.[28] The basic advantage of this method is the possibility to add the self-consistent calculated van der Waals forces to the Hellmann-Feynman ones to fully relax the molecule-surface system. We previously emphasized the importance of the inclusion of these dispersion forces to obtain

a reliable adsorbate-substrate geometry in the case of the pyridine adsorbed on Cu(110) and Ag(110) surfaces[29] or in the case of a N,N′-di(*n*-butyl) quinacridone monolayer on the Ag(110) substrate.[30] A similar semi-empirical approach was used to study the interaction of adenine with graphite(0001) surface[31] or applied to noble-gas, N_2 and benzene dimers.[32] Additionally, the energetics of the thymine-Cu(110) substrate was analyzed by means of the seamless approach (vdW-DF) proposed by Dion*et al.*[33] In this *ab initio* method, the vdW interactions are evaluated in a non-self-consistent procedure as a nonlocal correlation energy functional. This approach was already employed to investigate, for instance, benzene, naphthalene and phenol on graphite(0001),[34,35] or thiophene on Cu(110) surfaces.[36]

III. RESULTS AND DISCUSSION

A. Thymine in gas phase

To analyze how the molecule-substrate interaction modifies the geometry of the adsorbed thymine ($C_5H_6N_2O_2$) on Cu(110) surface, we first optimized the geometry of this molecule in the gas phase [see Fig. 1(a)]. The structural optimization was performed by using a cubic unit cell of $20\times20\times20$Å^3. The calculated bond lengths and bond angles are reported in Table I. For comparison, in this table we also list the data of similar DFT calculations performed in Ref. 37. Overall, one can observe that both studies provide a similar description of the molecular geometry.

Similarly, the first step in understanding the electronic structure of the thymine-surface interface is to analyze the electronic structure of the $C_5H_6N_2O_2$ molecule in the gas phase. Therefore, in Fig. 4(a) we present the corresponding angular-momentum resolved local density of states (LDOS). The highest occupied molecular orbital (HOMO) as well as the lowest unoccupied molecular orbital (LUMO) are π-like molecular orbitals, originating mainly from the atomic p orbitals perpendicular on the molecular plane (pyrimidine ring, consisting of C and N atoms). The molecular orbital HOMO-1 and HOMO-2 have a σ character indicating that the chemical bonding takes place in the molecular plane.

B. Ground-state geometry and energetics

1. *Perpendicular adsorption geometry*

Without vdW interactions – To explore the possibility to chemically functionalize the Cu(110) surface via the adsorption of a single thymine molecule on it, in our study we investigated several perpendicular adsorbate-substrate geometries. In all these adsorption configurations, the thymine binds to surface via the N atom after a deprotonation process involving a N–H bond breaking.

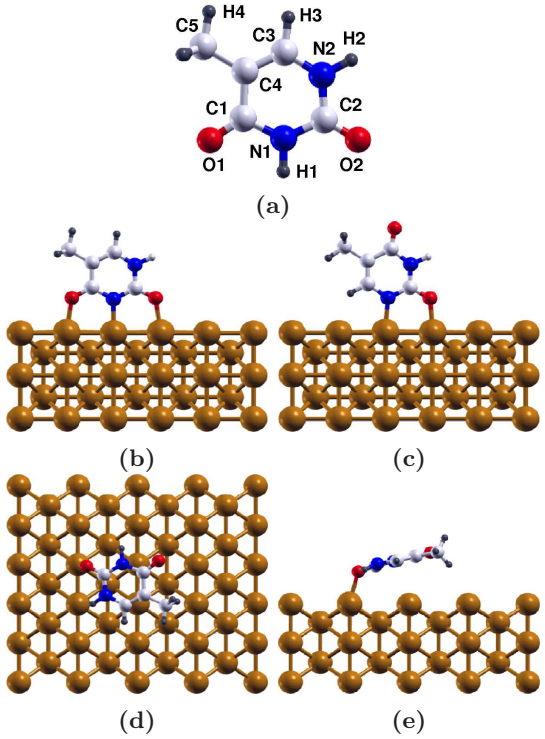

FIG. 1: **(a)** Ball-and-stick model of the thymine molecule in the gas phase. **(b)** In the ground-state, the thymine molecule adsorbs on the Cu(110) surface via three bonds (N1–Cu,O1–Cu,O2–Cu) with the molecular plane perpendicular to surface and oriented along the $[1\bar{1}0]$ surface direction. This adsorption configuration is labeled as ONO–H in Table II. An additional adsorption geometry obtained by removing the hydrogen atom colored in grey (H2 in **(a)**) was also investigated (denoted as the geometry ONO–H_2 in Table II). **(c)** Alternatively, the thymine can attach to Cu(110) surface via two chemical bonds (N2–Cu and O1–Cu). For this configuration one can consider also the cases of a single (NO–H geometry in Table II) or a double (NO–H_2 in Table II) deprotonated thymine molecule. **(d)** Top and **(e)** lateral view of the most stable configuration of a parallel geometry of thymine on Cu(110). The O1–O2 "bond" line is oriented parallel to [001] surface direction. The plots presented in the present work have been obtained by using XCrysDen.[38]

A binding of thymine on the Cu(110) substrate through a N atom is similar to the pyridine on Cu(110) and Ag(110) surfaces.[29]

However, in the case of the thymine-Cu(110) system, there are two different possible bonding N atoms denoted as N1 and N2 in Fig. 1(a). The molecule-surface geometry corresponding to the adsorption through the N1 atom is presented in Fig. 1(b) (hereafter referred to as ONO–H configuration) and that corresponding to the bonding via the N2 atom is depicted in Fig. 1(c) (hereafter referred to as NO–H configuration). In both cases, the molecular plane given by the pyrimidine ring is oriented along the $[1\bar{1}0]$ surface direction. In the present work we also investigated the case when the molecular plane is paral-

	Gas phase		Cu(110)		
	this work	Ref. 37			
Configuration			Perpendicular	Parallel	
Orientation			$[1\bar{1}0]$	$[1\bar{1}0]$	[001]
			DFT	DFT+vdW	
Bond Length (Å)					
C1-O1	1.232	1.222	1.266	1.232	1.229
C2-O2	1.229	1.218	1.262	1.248	1.251
C1-N1	1.412	1.408	1.376	1.427	1.430
C2-N1	1.385	1.386	1.356	1.372	1.369
C2-N2	1.392	1.390	1.379	1.375	1.370
C3-N2	1.375	1.380	1.367	1.378	1.379
C3-C4	1.358	1.352	1.360	1.363	1.362
C4-C5	1.511	1.501	1.511	1.508	1.506
C4-C1	1.479	1.468	1.468	1.473	1.475
N-Cu			1.988		
O1-Cu			2.017		
O2-Cu			2.028	2.218	2.135
Bond Angle (°)					
O1-C1-N1	119.9	120.4	120.8	119.6	119.6
O2-C2-N1	124.5		124.8	123.8	122.9
C1-N1-C2	128.6	128.3	121.6	127.8	127.6
C2-N2-C3	124.2	123.9	122.8	123.1	123.2
N2-C3-C4	122.9	122.7	121.1	123.2	122.8
C3-C4-C5	123.8	124.1	123.1	123.5	123.8
C3-C4-C1	117.8	118.2	116.7	117.7	118.0
C4-C1-O1	125.9		119.5	126.5	126.5
C4-C1-N1	114.2	114.5	119.7	113.9	113.8

TABLE I: The bond lengths and bond angles calculated for the thymine molecule in gas phase and adsorbed on Cu(110) surface. In the case of a perpendicular adsorption geometry, only the values obtained for the ground state [see Fig. 1(b)] are presented. In the case of a parallel adsorption geometry, only the data of the most stable configurations are reported. In particular, the geometry corresponding to the orientation [001] is sketched in Fig. 1(d). In the orientation $[1\bar{1}0]$, the O1–O2 "bond" line is oriented parallel to this surface direction. The atomic labels are those indicated in Fig. 1(a).

lel to the [001] surface direction. Additionally, for each adsorption geometry already mentioned, we considered the possibility that the $C_5H_6N_2O_2$ molecule on Cu(110) surface is double deprotonated, i.e., both N–H bonds are broken.

To determine which adsorption configuration is energetically the most favorable one, we compared the corresponding adsorption energies reported in Table II. One can easily observe that, for all perpendicular thymine-surface configurations considered in our study, in the ground-state adsorption geometry the molecular plane is oriented parallel to $[1\bar{1}0]$ direction. Also, a lower adsorption energies is obtained for the ONO–H adsorption configuration than for the NO–H one and a similar conclusion is drawn for the ONO–H_2 geometry when compared with the NO–H_2 one. This behavior is not surprising since early studies of formate[40] and terephthalic acid[41] on Cu(110) surface revealed that the oxygen atoms of these molecules adsorb on top of the surface atoms. As clearly shown in Fig. 1(b) and (c), in the case of the $[1\bar{1}0]$ adsorption geometries, both thymine oxygen atoms lie above the surface Cu ones. One the other hand, in the case of the ONO–H (ONO–H_2) configurations there are two oxygen atoms above the surface one, in contrast to the case of the NO–H (NO–H_2) geometries where only one oxygen atom interacts directly with the surface.

Also, the calculated adsorption energies for the geometries with a double deprotonated thymine on the Cu(110) substrate are lower than those obtained for the single deprotonated adsorption configurations. However, since for these adsorbate-surface geometries the number of atoms is different, it is not possible to compare directly the corresponding adsorption energies to infer which configuration is the most stable one. However, by comparing the calculated adsorption enthalpies $\Delta H^{ads}_{T=0}$ one can determine if the deprotonation process of thymine molecule is favorable from energetic point of view or not. In particular, this information is of peculiar importance for a dou-

geometry	orientation	adsorption energy E_{ads} (eV) DFT(PBE)	DFT-D	vdW-DF PBE	vdW-DF revPBE	adsorption enthalpy $\Delta H^{ads}_{T=0}$ (eV) DFT(PBE) Eq. 2	DFT(PBE) Eq. 3	DFT(PBE) Eq. 4	DFT-D Eq. 2	DFT-D Eq. 3	DFT-D Eq. 4
					Perpendicular						
ONO-H	$[1\bar{1}0]$	−3.666	−4.011	−4.078	−3.613	−0.618			−0.621		
	[001]	−3.027	−3.396	−3.566	−3.157	+0.022			−0.006		
ONO-H_2	$[1\bar{1}0]$	−4.643	−4.994	−5.091	−4.623	+0.832	+1.450	−2.217	+0.822	+1.443	−2.510
	[001]	−3.902	−4.282	−4.438	−3.994	+1.573	+1.551	−1.475	+1.535	+1.540	−1.800
NO-H	$[1\bar{1}0]$	−2.674	−3.050	−3.042	−2.668	−0.064			−0.098		
	[001]	−2.561	−2.960	−2.987	−2.610	+0.048			−0.007		
NO-H_2	$[1\bar{1}0]$	−3.160	−3.590	−3.570	−3.198	+2.316	+2.380	−0.294	+2.228	+2.326	−0.578
	[001]	−3.136	−3.510	−3.591	−3.208	+2.340	+2.292	−0.270	+2.307	+2.314	−0.450
					Parallel						
flat	$[1\bar{1}0]$	+0.296	−0.260	−0.516	−0.002	−			−		
	[001]	+0.112	−0.319	−0.703	−0.247	−			−		

TABLE II: The adsorption energies E_{ads} and adsorption enthalpies $\Delta H^{ads}_{T=0}$ for the thymine–Cu(110) adsorption geometries considered in our study [see Fig. 1(b), (c), (d) and (e), respectively]. Here DFT(PBE) denotes the first-principles DFT results obtained with the PBE[22] exchange-correlation energy functional, DFT-D represents the DFT results plus the semiempirical vdW contribution as proposed by Grimme[28] and vdW-DF implies the DFT results obtained by using the Dion[33] functional. Note that in the case of the vdW-DF calculations we employed PBE[22] as well as revPBE[39] exchange-correlation energy functionals.

ble deprotonated thymine since in this case the $\Delta H^{ads}_{T=0}$ and the relative surface free energies $\Delta\gamma$ plotted as a function of the chemical potential μ_H of the H atom will allow us to determine which reaction path corresponding to Eq. 2, Eq. 3 or to Eq. 4 is the most probable one.

In the light of the above considerations, from Table II one can deduce that for a single deprotonated thymine molecule on Cu(110) surface (ONO–H and NO–H configurations) the ground-state $[1\bar{1}0]$ adsorption geometry does not require external energy to deprotonate the $C_5H_6N_2O_2$ molecule, in contrast to the [001] configuration.

In the case of a double deprotonated molecule, the large adsorption energy which is a measure of the binding strength suggests that the double deprotonated species might coexists together with single deprotonated species on the metal surface. An important question is how a double deprotonated species would arise. In our study we considered three different scenarios for a double deprotonation process:
(i) the reaction path suggested by Eq. 2 implies an instantaneous double deprotonation process when the thymine adsorbs on the Cu(110) surface. This could take place at high temperatures since the reaction is endoterm (requires external energy to take place);
(ii) the reaction path described by Eq. 3 implies that the single deprotonated thymine adsorbed on the Cu(110) loses instantaneously its second hydrogen yielding a double deprotonated species adsorbed on the surface. This process is also an endothermic one and requires a larger amount of energy to take place as compared to (i);
(iii) the Eq. 4 assumes a reaction path in which a single deprotonated thymine molecule in gas phase adsorbs on the metal substrate where it undergoes a second deprotonation process. Since a large amount of energy is released, the adsorption process is an exotherm one and the probability to occur is can be significant (depending on the hight of the energy barrier of the transition state).

Since the adsorbed species of the flat thymine, ONO–H and ONO–H_2 differ only through the number of hydrogen atoms, in Fig. 2 we have plotted the relative surface free energies $\Delta\gamma$ as a function of the chemical potential μ_H of the H atom. Details of how $\Delta\gamma$ was calculated are presented in Appendix. At a given temperature, the chemical potential of the H atom can be expressed in terms of the H_2 molecular pressure which together with the temperature represent the parameters used in experiments to control which conformation of the thymine (single or double dehydrogenated) is adsorbed on the Cu(110) surface. The most stable configuration is the one that minimizes the relative surface free energy $\Delta\gamma$. In consequence, the Fig. 2 indicates that, independent on the temperature, the most stable configuration is ONO–H for the chemical potentials of the H atom between −0.9 and 0.0 eV. Note that these values correspond to the chemical potential interval in which the experiments can be performed. However, the experiments[17,18,19,20] indicate that by preparing the sample at 300 K the ONO-H species are present on the surface while when increasing the temperature higher than 500 K the ONO-H_2 species are predominat at an experimental pressure of 10^{-12} atm. Based on the the experimental observations and as shown by our *ab initio*

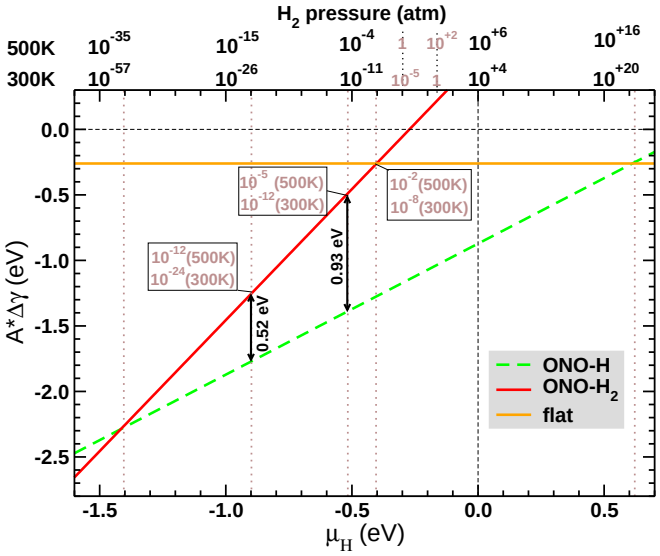

FIG. 2: Relative surface free energies $\Delta\gamma$ of the flat, ONO–H and ONO–H_2 configurations as function of the H chemical potential μ_H. The values of the $\Delta\gamma$ are normalized by the surface area A of the unit cell (see Appendix). At the top of the $x-$axis, the chemical potential of the H_2 molecule μ_{H_2} is given as a pressure scale at two fixed temperatures: 300 K and 500 K.

calculations (see Fig. 2) we conclude that at room temperature ($\approx$ 300 K) there is a high activation energy between ONO–H and ONO–H_2 adsorbed species and therefore the second deprotonation process cannot take place. Increasing the temperature over 500 K this energetic barrier can be overcome such that the ONO-H_2 species are formed.[20]

To conclude, our first-principles calculations suggest that a double deprotonated thymine molecule adsorbed on Cu(110) surface can be formed only at high temperatures as follows: (i) the thymine adsorbs on the Cu(110) surface undergoing an instantaneous double deprotonation process (see Eq. 2)or (ii) the single deprotonated thymine adsorbed on the Cu(110) loses its second hydrogen yielding a double deprotonated species adsorbed on the surface (process described by Eq. 3). Note that even if the adsorption enthalpy calculated for the deprotonation process described by Eq. 4 is negative and thus this process is exothermic, a single deprotonated pyridine molecule in gas phase requires to be desorbed from the Cu(110) surface. In consequence, to initialize this process one needs to provide an amount of externel energy that equals at least the adsorption energy of the ONO-H or NO-H configurations and therefore this scenario is less probable than those described by Eqs. 2 and 3.

Role of the vdW interactions – When including the van der Waals interactions using the DFT-D approach, all relaxed thymine-Cu(110) geometries considered in our study remain practically the same as those obtained without including the effect of the dispersion corrections. This outcome of our *ab initio* calculations is not surprising since in all perpendicular adsorption configurations the thymine molecule form a chemical bond with the surface via a N atom. As already discussed by Thonhauser *et al.*,[42] for covalently bonded systems like a CO_2 molecule or the bulk silicon, the inclusion of the vdW interactions does not alter the geometry obtained by DFT calculations.

However, the dispersion corrections will generally lower the adsorbtion energy of an adsorbate-substrate system. The importance of this effect for chemisorbed systems was emphasized in the study of the adsorption mechanism of benzene on Si(001) surface performed by Johnston *et al.*[43] Their first-principles calculations based on the vdW-DF approach[33] revealed that the PBE and revised PBE (revPBE)[39] calculations predict a different ground-state geometry than the vdW-DF ones. Therefore, to take into account the weak vdW interactions might be important even for the strongly chemisorbed molecule-surface systems. As presented in Table II, in the case of thymine-Cu(110) surface the $[1\bar{1}0]$ adsorption geometry remains the ground-state one for all four adsorption configurations even in the presence of the attractive van der Waals interactions. In the semi-empirical (DFT-D) approach, their main effect is to lower the adsorption energy calculated for the perpendicular adsorbate-surface geometries by about 0.3 eV with respect to the values obtained with PBE. Note that this energy gain due to the dispersion corrections is similar to that obtained for pyridine on Cu(110) and Ag(110) surfaces.[29] As regarding the adsorption enthalpies, their values are also lowered when the dispersion effects are included.

A final note of this section concerns the comparison of the adsorption energies obtained with the semi-empirical (DFT-D) and seamless (vdW-DF) methods, the latter values being obtained with a code developed by us.[44] We briefly remind that in the vdW-DF approach the correlation part of the GGA functional is replaced by a sum of the LDA correlation functional $E_{LDA,c}$ and a nonlocal term E_c^{nl}:

$$E_{vdW-DF} = E_{GGA} - E_{GGA,c} + E_{LDA,c} + E_c^{nl}. \quad (5)$$

where E_{GGA} is the self-consistent GGA total energy E_{GGA} evaluated in a conventional DFT calculation. The nonlocal correlation energy E_c^{nl} can be expressed as a function of the charge density $n(\boldsymbol{r})$

$$E_{\rm c}^{\rm nl} = \frac{1}{2}\int\int d\boldsymbol{r}d\boldsymbol{r'}n(\boldsymbol{r})\phi(\boldsymbol{r},\boldsymbol{r'})n(\boldsymbol{r'}). \quad (6)$$

where the kernel function $\phi(\boldsymbol{r},\boldsymbol{r'})$ is discussed in detail in Ref. 33. Note that in our study we employed both PBE and revPBE flavours of the GGA exchange-correlation energy functional.

From Table II it becomes apparent that in the case of the perpendicular adsorption geometries, the vdW-DF values calculated with PBE are in excellent agreement with those obtained by using the semi-empirical

approach DFT-D. This observation leads us to the preliminary conclusion that, in the case of the covalently bonded systems, the DFT-D and vdW-DF will provide similar results based on the PBE functional. However, when using the revPBE, the adsorption energies calculated with the vdW-DF approach are higher by ≈0.3 eV that those obtained with DFT-D method based on PBE. This behaviour is similar to that observed for chemisorption energy of atoms and molecules on transition-metal surfaces as pointed out by Hammer *et al.*[45]

2. *Parallel adsorption geometry*

Role of the vdW interactions – In our study we also focused on the thymine-Cu(110) surface interaction when the molecule lies flat on the substrate. More specifically, we considered two different adsorption configurations such that the molecule is oriented with the line given by O–N–O along [001] direction ([001] geometry) or along [1$\bar{1}$0] one ([1$\bar{1}$0] geometry). Intuitively, in these adsorption configurations the molecule-surface bonding mechanism implies an interaction between a π molecular orbital and surface states which eventually leads to a weakly bonded system. As was already discussed in literature for benzene and naphthalene molecules on graphite(0001),[34] phenol on graphite(0001) and α-Al_2O_3(0001)[35] or for thiophene on Cu(110) surfaces,[36] the van der Waals correlations play a crucial role to correctly describe the energetics of such systems.

Indeed, the PBE calculations performed for both flat geometries predict an average molecule-substrate distance of ≈3.4 Å that is a clear fingerprint of a physisorption process. However, by including the dispersion effects and relaxing the adsorbate-substrate interface, in both configurations the molecule-surface distance drops to ≈2.7 Å. Besides this, the thymine becomes tilted with respect to the surface by an angle of ≈111° and ≈104° for [001] and [1$\bar{1}$0] geometries, respectively. This behavior is similar to that observed for pyridine on Cu(110) and Ag(110) surfaces[29] and clearly emphasizes the importance of taking into account the structural relaxations for such weakly bonded molecule-surface systems. From bonding point of view, the main difference with respect to the perpendicular adsorption configurations is that a flat thymine molecule is anchored to Cu(110) via a O–Cu bond with a bondlength of ≈2.1 Å.

The necessity to include the dispersion corrections when investigating van der Waals systems is illustrated by the analysis of the calculated adsorption energies. As shown in Table II, the PBE calculations predict actually a *non-bonding* thymine-surface configuration since the adsorption energies are positive. However, when considering the effect of the van der Waals interactions on the semi-empirical level, these energies are lowered on average by ≈0.5 eV and become negative, denoting that a flat adsorption geometry of thymine on Cu(110) substrate is possible. In this case the [001] adsorption geometry is more stable than the [1$\bar{1}$0] one.

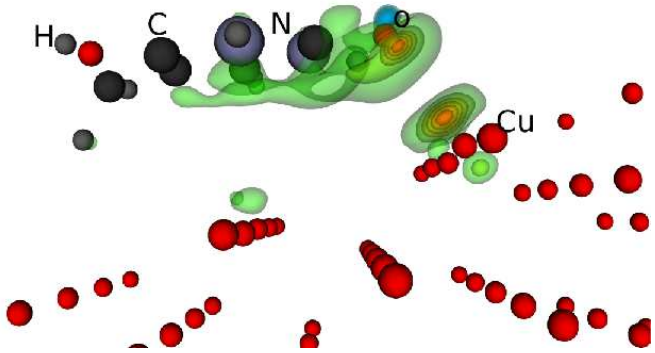

FIG. 3: (Color online) Perspective 3D-view of the the nonlocal correlation energy difference ΔE_c^{nl} of the thymine-Cu(110) surface system with respect to its isolated surface and molecule components. The red color shows regions with a large contribution to the binding energy while the green color represents regions with a much smaller contribution.

The use of the vdW-DF method does not qualitatively change the physical picture highlighted above. From quantitative point of view, the vdW-DF adsorption energies obtained with the PBE functional are lower by a factor of ≈2 with respect to those evaluated with the DFT-D approach. Similarly to the case of the perpendicular thymine-surface geometries, the vdW-DF adsorption energies calculated with the revPBE are about ≈0.5 eV higher then their PBE counterparts. Although the relative stability of the flat adsorption geometries considered in our study is not changed with respect to the PBE or the semi-empirical method, the use of revPBE leads to a very small value of the adsorption energy in the case of the [1$\bar{1}$0] configuration. This is consistent with the general tendency of the revPBE functional to provide theoretical chemisorption energies higher than the PBE one and thus presumably closer to the corresponding experimental values.[45] However, note that the revPBE does not generally lead to an overall better physical description than the PBE functional. For instance, in the case of a typical van der Waals system such as Kr dimer[46] while the depth of the Kr-Kr interaction potential is better described by revPBE, the equilibrium distance of this dimer is better reproduced by the PBE functional.

Since we applied the vdW-DF method to an initially weakly bonded system that in the final relaxed configuration exhibits a chemical bond, it is interesting to determine the role of the nonlocal correlation effects in this case. Therefore in Fig. 3 we present a plot of the difference in the nonlocal correlation energy due to the adsorption process, i.e., we map in real space the quantity $\Delta E_c^{nl} = E_c^{nl,sys} - E_c^{nl,Cu(110)} - E_c^{nl,thymine}$. The peculiar

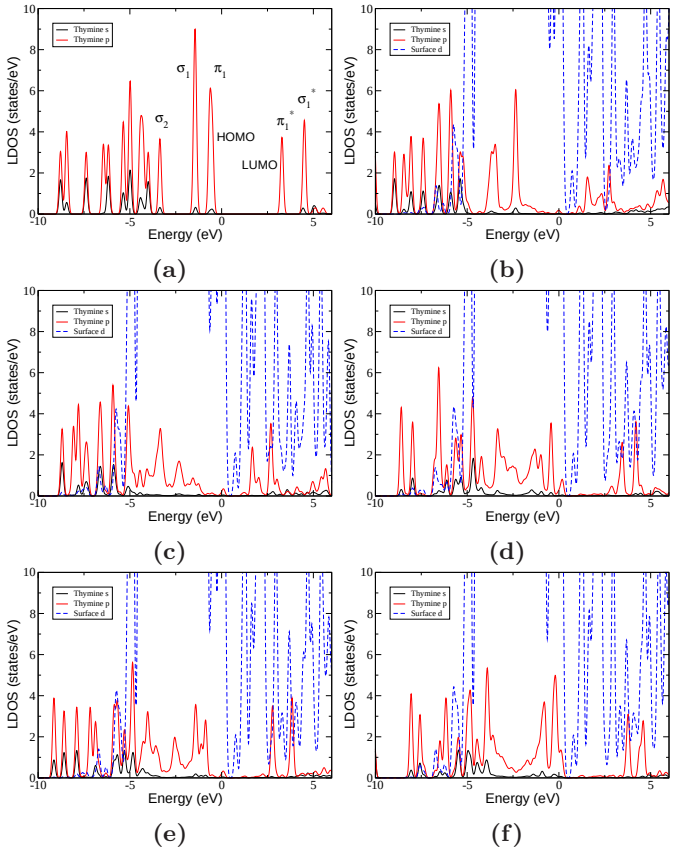

FIG. 4: Local density of states (LDOS) calculated for **(a)** the thymine in the gas phase, for **(b)** a flat thymine-surface adsorption geometry [see Figs. 1(d) and (e)]and for the **(c)** ONO-H, **(d)** ONO-H_2, **(e)** NO-H and **(f)** NO-H_2 perpendicular adsorption geometries of the $C_5H_6N_2O_2$ molecule on Cu(110) surface.

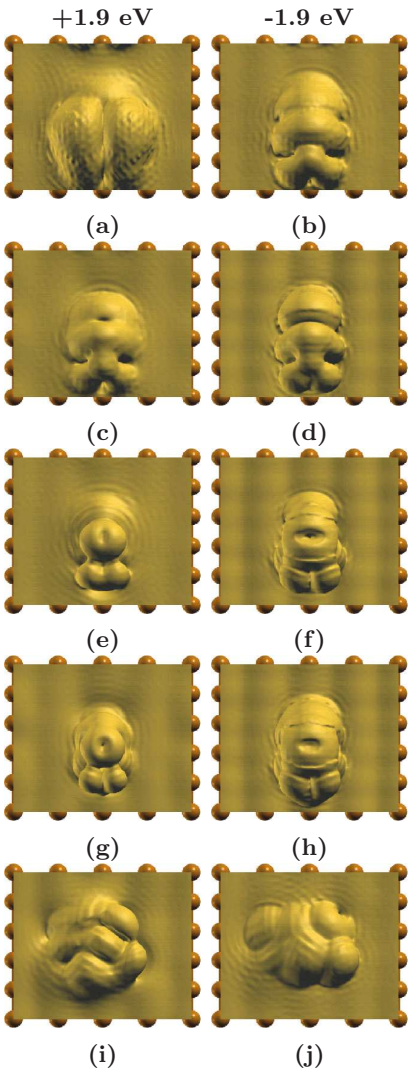

FIG. 5: The simulated STM topographies for **(a,b)** ONO–H, **(c,d)** ONO–H_2, **(e,f)** NO–H and **(g,h)** NO–H_2 perpendicular adsorption configurations. The similar images for a flat adsorption geometry [see Fig. 1(d) and (e)] are shown in **(i)** and **(j)**. The applied bias voltages are +1.9 and -1.9 eV, respectively. At a positive applied bias voltage the electrons will tunnel from the STM tip to the unoccupied electronic states of the molecule-surface interface.

feature displayed by this image is a strong contribution of the nonlocal effects to the bonding energy arising from the charge density $n(\boldsymbol{r})$ close to the O and Cu atoms that form a chemical bond. Qualitatively this behavior can be understood by noticing that to form a chemical bond between the O and Cu atoms, the charge density will shift from these atoms to the space between them. Therefore, they become polarized which favors a significant contribution of the nonlocal correlation energy given by Eq. 6 to the binding energy of the thymine-Cu(110) system.

C. Electronic structure

The calculated atom-projected local density of states (LDOS) for all adsorption configurations are presented in Fig. 4. A general feature of the electronic structure of all perpendicular adsorption geometries considered in our study is a strong hybridization of the highest occupied molecular orbitals (HOMOs) with the *d*-states of the Cu(110) surface in an energy range of 5 eV below the Fermi level. This strong molecule-surface interaction leads to broad bands with a mixed molecular-metal character. Besides this, in the energy range from -5 to -10 eV, the interaction of the molecular states with *s*- and *p*-states of the substrate become also important. As regarding the most stable flat adsorption geometry depicted in Fig. 1(d), its electronic structure also involves mainly a strong hybridization of HOMOs with the *d*-states of the substrate.

However, in an energy range of ±2 eV around Fermi level, the LDOS has specific features for each studied adsorption configuration. This observation is important

since the electronic structure of adsorbate-metal surface in this energy range can be probed by using the scanning tunneling microscope (STM). Therefore, using the Tersoff and Hamann theory,[47] we simulated maps of constant current for the ground-state perpendicular and parallel adsorption geometries considered in our study. The theoretical STM topographies are depicted in Fig. 5 for two different applied bias voltages. In general, the simulated STM images exhibit peculiar features for each adsorbate-surface configuration at each value of the bias voltage except for the NO–H and NO–H_2 geometries which exhibit similar features.

Among the simulated theoretical STM images, those obtained for the ONO–H geometry at a bias voltage of ± 1.9 eV present the most significant topographic difference. Also, except for this configuration, the simulated images suggest the possibility to obtain a sub-molecular resolution for single or double deprotonated thymine molecule adsorbed in a perpendicular configuration on Cu(110) surface. For instance, the methyl group (CH_3) appears as a distinct clear feature, especially in the case of the ONO–H_2 and NO–H geometries although its geometrical form is specific for each configuration in question. A similar sub-molecular resolution of the STM images is observed for a parallel adsorption geometry corresponding to the configuration shown in Fig. 1(d).

IV. SUMMARY

By using the *ab initio* pseudopotential method, we analyzed the adsorption process of a single thymine molecule on the Cu(110) surface. To determine the ground-state adsorption geometry, we investigated several adsorbate-substrate configurations such that the molecular plane is perpendicular or parallel to the (110) surface. To explore the possibility to chemically functionalize this molecule-surface system, for the perpendicular adsorption geometry we considered the case of a single and double deprotonated thymine molecule anchored to surface via different functional groups. Our *ab initio* simulations indicate that the strongest thymine-surface interaction takes place when the heterocycle ring is perpendicular to substrate and aligned along its $[1\bar{1}0]$ direction. For this ground-state adsorption geometry, the bonding of thymine on Cu(110) surface is due to a strong hybridization of the highest occupied molecular orbitals (HOMOs) with the *d*-states of the substrate. In the case of a flat adsorption geometry, our calculations demonstrate that the long-range van der Waals interactions play a very important role from both geometrical and energetic point of views. The effect of the dispersion corrections on the geometry of the relaxed adsorbate-surface interface was determined by using a semi-empirical approach. If the relaxed geometry obtained from PBE calculations remains almost parallel to surface, the inclusion of the van der Waals interactions leads to tilted adsorption geometry by an angle of 104°. Moreover, the van der Waals corrections have a more dramatic impact on the calculated adsorption energies. The PBE adsorption energies obtained for the flat adsorption geometries are positive and thus the PBE calculations suggest a *non-bonding* molecule-surface configuration. On the contrary, the adsorption energies calculated with the semi-empirical and the vdW-DF methods are negative and thus the parallel adsorption configuration becomes *bonding*. In this case the inclusion of the van der Waals interactions significantly modifies the character of the adsorption process from physisorption to chemisorption. As a final remark, we also simulated the scanning tunneling microscopy (STM) topography of the thymine-Cu(110) surface that can serve to distinguish in experiments between various adsorption configurations of the thymine-Cu(110) interface.

Acknowledgments

The computations were performed with the help of the JUMP and Blue/Gene supercomputers at the Forschungszentrum Jülich, Germany. We acknowledge the financial support from the DFG (Grants No. SPP1243 and No. HO 2237/3-1), Alexander von Humboldt foundation and Japan Society for the Promotion of Science. V.C., N.A. and P.L. thank to H. Hölscher, J.-H. Franke, H. Fuchs (University of Münster), K. Schroeder (Research Center Jülich) and R. Brako (Rudjer Bošković Institute) for many fruitful discussions and continuing support.

Appendix

A detailed description of how to evaluate the surface free energies using the total energies obtained from DFT calculations can be found in Refs. 48 and 49. In the following we will derive the equations used in the present work to calculate the relative surface free energies $\Delta\gamma$ plotted in Fig. 2.

For a deprotonation process characterized by the relative Gibbs free energy ΔG^{ads}, the relative surface free energy ($\Delta\gamma$) can be written as

$$\Delta\gamma = (1/A) * (\Delta G^{ads} + factor * \mu_H).$$

where A represents the surface area of the unit cell and μ_{H_2} is the chemical potential of the H_2 molecule. The $factor$ is equal 0.0 for thymine molecule, 1.0 for a single deprotonated or to 2.0 for a double deprotonated thymine molecule.

Assuming that the entropic term is small as compared to the values of the adsorption entalpies at $T = 0$ K,[49] we approximate ΔG^{ads} by $\Delta H^{ads}_{T=0}$. Therefore, the relative surface free energies $\Delta\gamma$ of the ground-state flat, ONO–H

and ONO–H_2 configurations are given by:

$$A * \Delta\gamma_{flat} \approx \Delta H^{ads}_{T=0} + 0.0 * \mu_H = -0.260 + 0.0 * \mu_H,$$
$$A * \Delta\gamma_{ONO-H} \approx \Delta H^{ads}_{T=0} + 1.0 * \mu_H = -0.872 + 1.0 * \mu_H,$$
$$A * \Delta\gamma_{ONO-H_2} \approx \Delta H^{ads}_{T=0} + 2.0 * \mu_H = +0.544 + 2.0 * \mu_H.$$

where μ_H has been calculated according to Eq. (22) from the Ref. 49 and the values of $\Delta H^{ads}_{T=0}$ correspond to those obtained with the DFT-D method.

* Electronic address: v.caciuc@fz-juelich.de
† Electronic address: n.atodiresei@fz-juelich.de

[1] C. W. Tang and S. A. VanSlyke, Appl. Phys. Lett. **51**, 913 (1987).
[2] J. S. (Ed.), *Organic Light-Emitting Devices* (Springer-Verlag New York, Inc., 2004), ISBN 0387953434.
[3] M. A. Reed, C. Zhou, C. J. Muller, T. P. Burgin, and J. M. Tour, Science **278**, 252 (1997).
[4] C. Joachim, J. K. Gimzewski, and A. Aviram, Nature **408**, 541 (2000).
[5] M. Elbing, R. Ochs, M. Koentopp, M. Fischer, C. von Hänisch, F. Weigend, F. Evers, H. B. Weber, and M. Mayor, Proc. Nat. Acad. Sci. USA **102**, 8815 (2005).
[6] M.-K. Ng, D.-C. Lee, and L. Yu, J. Am. Chem. Soc. **124**, 11862 (2002).
[7] I. I. Oleynik, M. A. Kozhushner, V. S. Posvyanskii, and L. Yu, Phys. Rev. Lett. **96**, 096803 (2006).
[8] C. D. Dimitrakopoulos, S. Purushothaman, J. Kymissis, A. Callegari, and J. M. Shaw, Science **283**, 822 (1999).
[9] C. Dimitrakopoulos and P. Malenfant, Adv. Mater. **14**, 99 (2002).
[10] V. C. Sundar, J. Zaumseil, V. Podzorov, E. Menard, R. L. Willett, T. Someya, M. E. Gershenson, and J. A. Rogers, Science **303**, 1644 (2004).
[11] J. E. Green, J. W. Choi, A. Boukai, Y. Bunimovich, E. Johnston-Halperin, E. DeIonno, Y. Luo1, B. A. Sheriff, K. Xu, Y. S. Shin, et al., Nature **445**, 414 (2007).
[12] D. S. Martin, R. J. Cole, and S. Haq, Phys. Rev. B **66**, 155427 (2002).
[13] D. S. Martin, R. J. Cole, and S. Haq, Surface Science **539**, 171 (2003).
[14] D. Ivnitski, I. Abdel-Hamid, P. Atanasov, and E. W. A. C. Information, Biosens. Bioelectron. **14**, 599 (1999).
[15] S. M. Radke and E. Alocilja, J. IEEE Sensors **5**, 744 (2005).
[16] Y. Liu, S. Chakrabartty, and E. C. Alocilia, Nanotech. **18**, 424017 (2007).
[17] A. McNutt, S. Haq, and R. Raval, Surface Science **502–503**, 185 (2002).
[18] T. Yamada, K. Shirasaka, A. Takano, and M. Kawai, Surface Science **561,**, 233 (2004).
[19] M. Furukawa, H. Fujisawa, S. Katano, H. Ogasawara, Y. Kim, T. Komeda, A. Nilsson, and M. Kawai, Surface Science **532–535**, 261 (2003).
[20] F. Allegretti, M. Polcik, and D. Woodruff, Surface Science **601**, 3611 (2007).
[21] P. Hohenberg and W. Kohn, Phys. Rev. **136**, B864 (1964).
[22] J. P. Perdew, K. Burke, and M. Ernzerhof, Phys. Rev. Lett. **77**, 3865 (1996).
[23] W. Kohn and L. J. Sham, Phys. Rev. **140**, A1133 (1965).
[24] M. C. Payne, M. P. Teter, D. C. Allan, T. A. Arias, and J. D. Joannopoulos, Rev. Mod. Phys. **64**, 1045 (1992).
[25] G. Kresse and J. Hafner, Phys. Rev. B **47**, 558 (1993).
[26] G. Kresse and J. Furthmüller, Phys. Rev. B **54**, 11169 (1996).
[27] P. E. Blöchl, Phys. Rev. B **50**, 17953 (1994).
[28] S. Grimme, J. Comput. Chem. **27**, 1787 (2006).
[29] N. Atodiresei, V. Caciuc, J.-H. Franke, and S. Blügel, Phys. Rev. B **78**, 045411 (2008).
[30] J.-H. Franke, V. Caciuc, L. F. Chi, and H. Fuchs, Phys. Rev. B **78**, 165432 (2008).
[31] F. Ortmann, W. G. Schmidt, and F. Bechstedt, Phys. Rev. Lett. **95**, 186101 (2005).
[32] F. Ortmann, F. Bechstedt, and W. G. Schmidt, Phys. Rev. B **73**, 205101 (2006).
[33] M. Dion, H. Rydberg, E. Schröder, D. C. Langreth, and B. I. Lundqvist, Phys. Rev. Lett. **92**, 246401 (2004).
[34] S. D. Chakarova-Käck, E. Schröder, B. I. Lundqvist, and D. C. Langreth, Phys. Rev. Lett. **96**, 146107 (2006).
[35] S. D. Chakarova-Käck, O. Borck, E. Schröder, and B. I. Lundqvist, Phys. Rev. B **74**, 155402 (2006).
[36] P. Sony, P. Puschnig, D. Nabok, and C. Ambrosch-Draxl, Phys. Rev. Lett. **99**, 176401 (2007).
[37] O. V. Shishkin, L. Gorb, and J. Leszczynski, Int. J. Mol. Sci. **1**, 17 (2000).
[38] A. Kokalj, J. Mol. Graphics Modelling **17**, 176 (1999).
[39] Y. Zhang and W. Yang, Phys. Rev. Lett. **80**, 890 (1998).
[40] N. Atodiresei, K. Schroeder, and S. Blügel, Phys. Rev. B **75**, 115407 (2007).
[41] N. Atodiresei, V. Caciuc, K. Schroeder, and S. Blügel, Phys. Rev. B **76**, 115433 (2007).
[42] T. Thonhauser, V. R. Cooper, S. Li, A. Puzder, P. Hyldgaard, and D. C. Langreth, Phys. Rev. B **76**, 125112 (2007).
[43] K. Johnston, J. Kleis, B. I. Lundqvist, and R. M. Nieminen, Phys. Rev. B **77**, 121404(R) (2008).
[44] P. Lazić, N. Atodiresei, M. Alaei, V. Caciuc, S. Blügel, and R. Brako, *submitted to Comp. Phys. Comm.*
[45] B. Hammer, L. B. Hansen, and J. K. Nørskov, Phys. Rev. B **59**, 7413 (1999).
[46] P. Lazić, R. Brako, and B. Gumhalter, J. Phys.: Condens. Matter **19**, 305004 (2007).
[47] J. Tersoff and D. R. Hamann, Phys. Rev. B **31**, 805 (1985).
[48] J. E. Northrup, Phys. Rev. B **44**, 1419 (1991).
[49] K. Reuter and M. Scheffler, Phys. Rev. B **65**, 035406 (2001).